# Numerical study of the flow around 25° Ahmed bodies with hybrid turbulence models

F. Delassaux, I. Mortazavi, V. Herbert, and C. Ribes

## 1 Introduction

The aim of this work is to explore the efficiency of different improved Reynolds-Averaged Navier-Stokes (RANS) and hybrid LES/RANS approaches to study the external aerodynamics related to ground vehicles. These computational techniques should be able to build a bridge between accuracy and robustness in order to compute complex high Reynolds number bluff-body flows like ground vehicle flows. Bluff body flows are characterized by separated regions, containing wide spectra of turbulent scales. These regions, especially in the wake behind the body, are responsible for the main part of the drag forces. An accurate computation of these areas is a difficult task. Recently, different hybrid/modified models as Scale-Adaptive Simulation (SAS) [7], Delayed Detached Eddy Simulation (DDES) [10] and Stress-Blended Eddy Simulation (SBES) [2] have been developed to take advantage from the RANS low computational time without totally loosing the accuracy of Large Eddy Simulation (LES) models [9]. In order to get the best setup, the grid design is as critical as the model influence. In this work SAS, DDES and SBES models with unstructured meshes are used to simulate the flow around 25° Ahmed bodies. Two geometries are considered in this work : a sharp and a rounded edges 25° Ahmed bodies. Comparing these two geometries is very interesting as, on one hand, they represent a complex flow detachment on the rear slant for the sharp edges case and on the other hand, this complexity can be sensibly smoothed by rounding appropriate edges of the same body. Moreover, the rounded edges on the sides of the body delay the onset of the longitudinal vortices compared to sharp edges, making more challenging the flow prediction in this area. Ashton et al. [3] and Guilmineau et

F. Delassaux · I. Mortazavi
Equipe M2N, CNAM Paris, 292 rue Saint-Martin, 75003 Paris, France
e-mail: francois.delassaux@ext.mpsa.com

V. Herbert · C. Ribes
Groupe PSA, Route de Gisy, 78943 Velizy-Villacoublay, France

al. [5] works show the superiority of hybrid methods over RANS models for the separation/reattachment prediction on the rear slant surface of the body. First, the numerical setup is validated on the very common sharp edges Ahmed body. Then, the flow topology of the rounded case is investigated. The rounded edges allow us to get closer to a real vehicle shape with smooth rounded edges at the back. Numerical results are compared with experimental data from La Ferte Vidame (LFV) wind tunnel carried out by Rossitto et al. [8].

## 2 Ahmed bodies, grid and setup description

### *2.1 Ahmed bodies description*

Two different shape of Ahmed bodies are studied: a sharp one [1] and a rounded one [8]. These bluff bodies are illustrated in Figure 1, on the left the Ahmed body with sharp edges and on the right, the Ahmed body with rounded edges at the roof junction and side edges (in blue). The radius of curvature of the afterbody is expressed as a percentage of the reference length and is equal to 10% [8]. Consequently, sharp and rounded edges case are respectively named $R_0S_0$ and $R_{10}S_{10}$ thereafter.

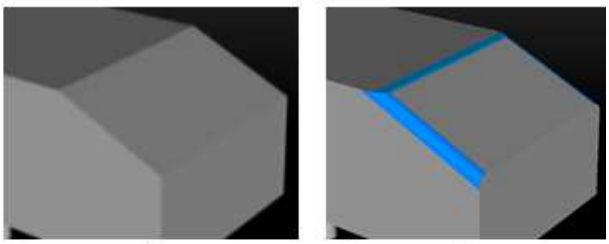

**Fig. 1** Ahmed body with sharp edges on the left and Ahmed body with rounded edges on the right

### *2.2 Grids and computational setup*

The computational domain is respectively $5L_B$ long upstream and $10L_B$ long downstream of the Ahmed body, with $L_B = 1,044m$, the length of the body. The cross section of domain is equal to $4.2L_B$ and its height is set to $5L_B$, giving a blockage ratio of $0,5\%$. The inlet boundary condition is defined as velocity inlet with $V_\infty = 40m/s$, yielding a Reynolds number based on the length of the model of $2.6 \times 10^6$. A pressure outlet condition is applied to the exit surface, with gauge pressure equal to 0

Pa. All the Ahmed body geometries are covered by no slip wall boundary condition. The ground of the computational domain is divided into two parts: from the inlet to $X/L_B = 3$, a slip wall condition is applied. For the remainder part of the ground, a no-slip wall condition is used to allow the build up of the boundary layer. The demarcation between these two parts allows to reproduce the experimental boundary layer thickness [8].

The near-wall regions are meshed with prisms. The others regions of the domain are fitted by tetrahedrons cells with box refinement in strategic locations of the flow (forebody, underbody and rear slant surface) to capture the separation/attachment phenomenon. The grids contain respectively, 22 and 19 million cells for sharp and rounded cases. The wall normal resolution is $y+ < 0.7$. In the streamwise and spanwise directions, the mesh is refined as $30 < \Delta s^+ = \Delta l^+ < 250$ for the rear slant, with a mean value as $\Delta s^+ = \Delta l^+ \approx 120$. More details on the grids can be found in [4]. Besides, the time step is fixed as $\Delta t = 5 \cdot 10^5 s$, ensuring a CFL number around 1 in critical areas of the flow. The computations were run for a total of 115 convective transit times defined as $T.V_\infty/L_B$, with $T = 3$ seconds of physical time. The time-averaging process was started after 77 transit times, to be sure of the relevance of the averaged quantities.

As for RANS models, $k-\omega$ SST [6] and SAS SST are used. The RANS $k-\omega$ SST is known to be one of the most accurate RANS model for the flow separation prediction. The SAS is an improved RANS formulation, which allows the resolution of a part of the turbulent spectrum in unstable flow conditions. DDES and SBES are called hybrid RANS/LES model. In these approaches, the unsteady RANS models are employed in the attached boundary layers, while the LES treatment is applied to the separated regions. These models differ from the shielding function used for the switch between RANS and LES [2], to protect the boundary layer from LES intrusion. Furthermore, with SBES, LES model is not embedded in RANS model, and any combination of RANS and LES models could be used.

## 3 Results and discussions

### *3.1* 25° *sharp edges Ahmed body - method validation*

On the sharp case, SAS, DDES and SBES approaches show relevant results for both drag and lift coefficients, as seen in Table 1. With an appropriate grid refinement, the DDES approach presents the best results compared to experiments and demonstrates the importance of capturing the shear layer due to separation on the backlight. Both drag and lift coefficient show a very good agreement with experiments, with an estimate error respectively of -2.5% and 3.8%.

One of the main feature of the flow around the 25° sharp edges Ahmed body is the closed recirculation bubble on the rear slant surface. The Figure 2 illustrates the zero-velocity contours of the longitudinal velocity $\overline{U_x} = 0$ for the three turbulence

**Table 1** Comparisons of drag and lift coefficients between experiments and numerical results on sharp edges Ahmed body

| Models | $C_d$ | $\Delta C_d\,[\%]$ | $C_l$ | $\Delta C_l\,[\%]$ |
|---|---|---|---|---|
| Experiments | 0.356 | - | 0.311 | - |
| SAS | 0.355 | - 0.3 | 0.298 | - 4.0 |
| DDES | 0.347 | -2.5 | 0.323 | 3.8 |
| SBES | 0.341 | - 4.2 | 0.328 | 5.4 |

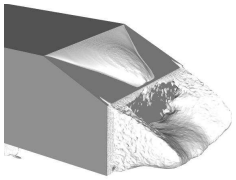

**Fig. 2a** SAS
$L_R = 100\%$

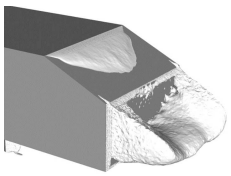

**Fig. 2b** DDES
$L_R = 75\%$

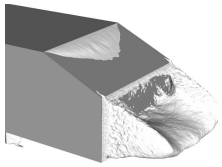

**Fig. 2c** SBES
$L_R = 53\%$

models studied. The length of the mean recirculation bubble from experiments $L_R$ is equal to 78% of the rear window length. The DDES model shows the best prediction for the mean recirculation bubble length, equal to 75%. SBES leads to a smaller closed recirculation bubble, with a recirculation length equal to 53%. On the contrary, SAS shows a reattachement at the end of the rear slant surface, so that $L_R$ is equal to 100% due to high modeled turbulent kinetic energy in the separation area. More results can be found in [4].

## *3.2* 25° *rounded edges Ahmed body*

Considering the rounded case, aerodynamical coefficients are drastically reduced as shown by experiments [8]. Drag and lift reductions, respectively of 16% and 18%, are observed. The Table 2 show the very good prediction of the three turbulence models for aerodynamic coefficients. The Figure 3 shows the Cp evolution along two different planes: the symmetry plane $Y/H = 0$ and $Y/H = 0,5$ with H the height of the body. The dashed line corresponds to the demarcation between the rear slant surface and the vertical base. It is clearly observable that the three turbulence models give very close results for both planes. For $0.9 < S^* < 1$, the flow acceleration due to the rounded edges lead to lower Cp values compared to sharp edges case. As the bubble reciruclation is suppressed, it results in pressure recovery over the slanted surface. This flow topology modification is directly responsible of drag reduction. Figure 4 shows Cp values in different cross-section planes from the top of the rear slant surface and the close wake. The left part of the figure is the sharp edges case and the rounded edges case is on the right. We can clearly observe the topology modification of the longitudinal vortices. Indeed, for the sharp case, the strength of

the vortices is significantly higher (lower Cp values) compared to the rounded case. Moreover, the onset of the longitudinal vortices is delayed leading to drag and lift forces reduction in this area of the flow.

**Table 2** Comparisons of drag and lift coefficients between experiments and numerical results on rounded edges Ahmed body

| Models | $C_d$ | $\Delta C_d$ [%] | $C_l$ | $\Delta C_l$ [%] |
|---|---|---|---|---|
| Experiments | 0.298 | - | 0.254 | - |
| SAS | 0.301 | 0.9 | 0.244 | - 4.0 |
| DDES | 0.299 | 0.4 | 0.251 | - 1.1 |
| SBES | 0.306 | 2.8 | 0.245 | - 3.7 |

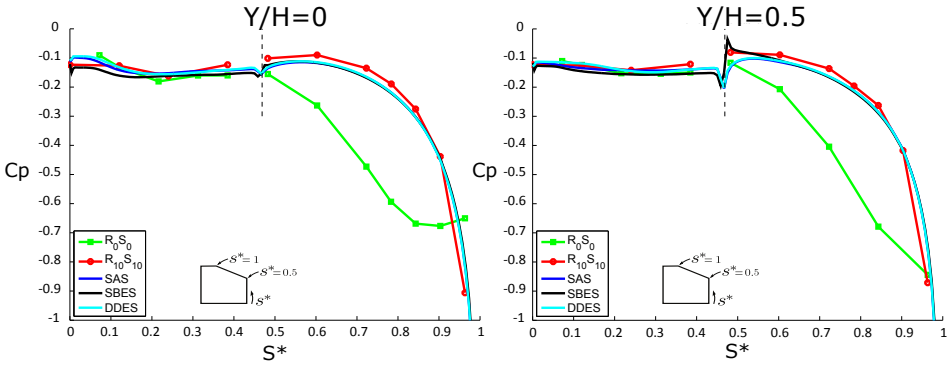


**Fig. 3** Pressure coefficient comparison between SAS, DDES and SBES models over the back of the body

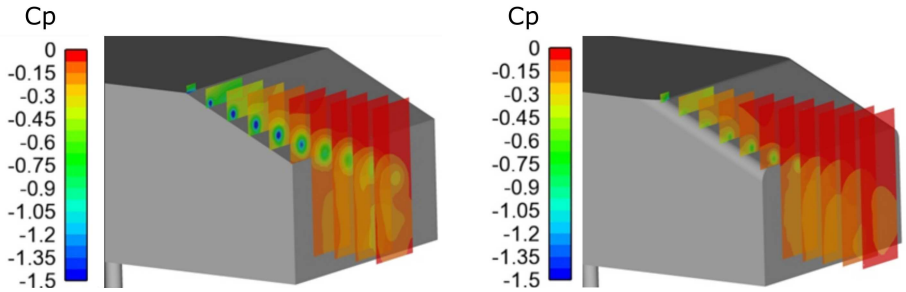


**Fig. 4** DDES evolution of pressure coefficient between sharp case (left) and rounded case (right) over cross-section planes

## 4 Conclusions

The flow topology around sharped edges and rounded edges Ahmed bodies has been investigated. For the sharp case, DDES model globally shows the best prediction for drag and lift coefficients with respectively errors around $-2.5\%$ and $3.8\%$. The size of the recirculation bubble, equal to 75% compared to 78% experimentally, is also very well predicted with DDES model. SAS seems to suffer in the vicinity of separation zone and acts like RANS models in this area. The higher level of turbulent kinetic energy (not shown here) compared to the two other turbulence models explain the longer recirculation bubble observed. For the rounded case, the DDES model shows again the best prediction for both drag and lift coefficient. The Cp values along two planes over the back of the body state that the three turbulence model give very good agreement with experiments. The Cp plots explain the flow topology modification between the two cases. Due to rounded edges at the transition between the roof and the rear slant surface, the flow separation disappears leading to pressure recovery all along the rear surface. The rounded edges on the sides of the body delay the onset of the longitudinal vortices and reduce their intensity. These two major modifications in the flow topology lead to drag and lift reduction. Globally, the main flow structures for both cases have been recovered using Hybrid RANS/LES models.

## References

1. Ahmed, S.R., Ramm, R. and Faltin, G.: Some salient features of the time-averaged ground vehicle wake, *SAE Technical Paper Series* **840300**, Detroit, (1984).
2. ANSYS Fluent Theory Guide, Release 17.0, (2016).
3. Ashton, N., West, A., Lardeau, S., Revell, A.: Assessment of RANS and DES methods for realistic automotive models, *Computers and Fluids*, **128**, 1–15, (2016).
4. Delassaux, F., Mortazavi, I., Herbert, V. and Ribes, C.: Comparison of three hybrid turbulence models for the flow around a 25 Ahmed body. Will be published In: Proceedings of the Symposium on 6th Hybrid RANS-LES Methods, Strasbourg, FRANCE (2017)
5. Guilmineau, E., Deng, G.B., Leroyer, A., Queutey, P., Visonneau, M., Wackers, J.: Assessment of hybrid RANS-LES formulations for flow simulation around the Ahmed body, *Computers and Fluids*, Article in Press, (2017).
6. Menter, F. R.: Zonal two equation k-$\varepsilon$ turbulence models for aerodynamic flows. *AIAA paper*, **2906** (1993).
7. Menter, F. R., Egorov, Y.: The scale-adaptive simulation method for unsteady turbulent flow predictions. Part 1: theory and model description. *Flow, Turbulence and Combustion*, **85(1)**, 113–138 (2010).
8. Rossitto, G., Sicot, C., Ferrand, V., Bore, J. and Harambat, F.: Influence of afterbody rounding on the pressure distribution over a fastback vehicle, *Experiments in Fluids*, **57:43**, (2016).
9. Sagaut, P.: Large eddy simulation for incompressible flows: an introduction, *Springer Science & Business Media*, (2006).
10. Spalart, P.R., Deck, S., Shur, M., Squires, K.D., Strelets, M., Travin, A.: A new version of detached-eddy simulation, resistant to ambiguous grid densities, *Theor. Comput. Fluid Dyn.*, **20**, 181–195, (2006).